Journal of Plant Pathology (2026) 108:895–910
https://doi.org/10.1007/s42161-026-02148-5

ORIGINAL ARTICLE

Soil conditions favoring basal stem rot infection in oil palm plantations

M. H. Ezrin[1] · **W. Aimrun**[1,2] · **S. K. Bejo**[1,2]

Received: 21 August 2025 / Accepted: 2 February 2026 / Published online: 17 March 2026
© The Author(s) 2026

Abstract

Basal Stem Rot (BSR), caused by *Ganoderma boninense* (*G. boninense*), poses a major threat to oil palm (*Elaeis guineensis*) cultivation in Malaysia, with serious implications for agricultural productivity and economic resilience. This study examines the relationship between soil physical and chemical properties and BSR incidence in two key plantation regions: Seberang Perak and Kluang. A total of 106 palm census points were assessed, where soil samples and BSR infection data were systematically collected. Key physical parameters such Cone Index (CI), moisture content, and elevation were measured alongside chemical properties such as pH, Cation Exchange Capacity (CEC), and nutrient levels (Mg, Ca, K, P, Cu, Zn, S, and C). Descriptive analysis indicated high site-dependent variability, particularly in phosphorus (P) and copper (Cu) in Seberang Perak, Perak and across most parameters in Kluang, Johor with coefficients of variation exceeding 30%. Independent t-tests revealed that magnesium (Mg) was the only nutrient significantly associated with BSR infection in both plantations. In Seberang Perak, additional significance was observed for CEC, P, and CI. Spatial interpolation highlighted distinct zones where low Mg levels aligned with high BSR infection. These findings suggest that soil magnesium content may serve as a robust early indicator for BSR risk, supporting the integration of soil nutrient mapping with precision agriculture approaches. Further research across diverse plantation environments is recommended to validate Mg as a BSR influencer and to inform soil-based strategies for sustainable oil palm cultivation.

Keywords Soil fertility · Oil palm disease · GIS mapping · Kriging method

Introduction

Oil palm (*Elaeis guineensis Jacq.*) remains a cornerstone of Malaysia's agricultural economy and one of the most important plantations crops globally. As of 2024, Malaysia's total oil palm planted area was approximately 5.61 million hectares, accounting for nearly 15% of the country's total land area (MPOB Malaysian Palm Oil Board 2024). The crop thrives in Malaysia's tropical soils, which are acidic (pH levels between 4 and 8), and can grow under various environmental conditions, with optimal growth at temperatures between 30 and 32 °C (Rozieta et al. 2015). However, oil palm plantations are increasingly facing significant challenges that affect their productivity and long-term sustainability. One such challenge is the occurrence of basal stem rot (BSR) caused by the *Ganoderma boninense* (*G. boninense*) fungus. BSR is a major threat to oil palm plantations, leading to severe economic losses, especially when it affects older plantations. In Malaysia, the disease has been observed in young plants and seedlings, a concerning development given its historical prevalence in older oil palms (Leng et al. 2024). This shift indicates an evolving challenge for disease management, as BSR can kill up to 80% of plants by the mid-point of their economic lifespan (Murphy et al. 2021).

The disease is particularly prevalent in areas with specific soil types, such as inland lateritic and peat soils, which may have previously been free of the infection. As the disease spreads, up to 50% of palms in a plantation can be lost by the time of replanting, with many others showing symptoms of infection. The distinctive symptoms of BSR,

✉ M. H. Ezrin
ezrin@upm.edu.my

[1] Smart Farming Technology Research Center, Universiti Putra Malaysia, UPM Serdang, Selangor 43400, Malaysia

[2] Department of Biological and Agricultural Engineering, Faculty of Engineering, Universiti Putra Malaysia, UPM Serdang, Selangor 43400, Malaysia

such as yellowish foliage, necrosis of older leaves, and the presence of fungal fruiting bodies on the trunk, are crucial for accurate diagnosis and monitoring in the field (Santoso et al. 2024). While oil palm can tolerate some flooding and waterlogging, the spread of BSR significantly reduces the palm's ability to thrive, making plantations vulnerable to declines in production and overall yield. The economic impact of this disease is substantial, particularly as oil palm remains a key revenue generator for Malaysia, with any significant reduction in productivity potentially having widespread consequences for the nation's economy (Nusaibah et al. 2016). As such, managing BSR and understanding its dynamics is critical to ensuring the continued success of oil palm cultivation. Recent studies confirm an increase in BSR incidence, particularly in second-generation plantations and newly replanted areas, with reported yield losses reaching up to 50% (Zakaria 2023). The disease spreads rapidly within one to two years after replanting, especially on land previously planted with perennial hosts such as coconut, highlighting the role of soil-borne inoculum persistence in disease development (Hardini et al. 2025).

Oil palms infected with BSR are asymptomatic in the early stages of the infection, with the earliest symptom frequently being noticed on foliage when the infection has developed by 60–70%. Young oil palm plants that exhibit disease symptoms typically die within 1 to 2 years, while mature trees only have a 3-to-5-year life expectancy (Khoo and Chong 2023). Disease symptoms on the old palms is clearer, the appearance of a number of spear leaves and collapse of old fronds are the main symptoms (Soepena et al. 2000). In Malaysia, the economic impact of this disease is profound, with estimates of up to US$ 500 million lost annually due to BSR (Zakaria 2023). While, the total economic impact for Indonesia's oil palm industry has been estimated at over USD 1 billion annually, reflecting its larger plantation area and higher overall production (Hushiarian et al. 2013). Projections indicate that the economic losses could rise significantly in the coming decades as the pathogen becomes more virulent and climate change exacerbates the conditions for its spread (Paterson 2019). Soil temperature and other environmental factors contribute to the spread of *G. boninense*, as its growth is facilitated in certain temperature ranges (Karunaratna et al. 2024). Climate change further complicates the issue, as rising temperatures are expected to create conditions more favourable to the fungus, thus threatening the long-term viability of the oil palm industry (Paterson 2019).

Infection by *G. boninense*, the causal agent of BSR in oil palm (*Elaeis guineensis*), can occur as early as the nursery or juvenile stages, although visible symptoms may not develop until several years later. Controlled inoculation studies have demonstrated that *G. boninense* infection can be established in seedlings as young as five-months-old, with pathogen colonization detectable by molecular and spectral techniques within five to ten months post-inoculation, even in the absence of external symptoms left from previous planting cycles, enabling latent infections that may persist undetected for long periods (Paterson 2022). Airborne basidiospores can also contribute to new infections, particularly during replanting operations where inoculum levels are high (Flood et al. 2022; Zakaria 2023).

Under plantation conditions, the first visible symptoms of BSR are most frequently observed between 4 and 8 years after planting, depending on site conditions, inoculum density, and management practices (Flood et al. 2022; Siddiqui et al. 2021). Typical early symptoms include unopened spears, chlorotic or desiccated lower fronds, and gradual canopy thinning, followed by the emergence of basidiocarps at the trunk base when internal colonization of the basal tissues exceeds approximately 60–70% (Khoo and Chong 2023). In heavily infested or poorly managed replanting sites, particularly on peat soils or high-moisture environments, symptomatic palms as young as two to three years old have been reported (Jazuli et al. 2022; Zakaria 2023). Once visible symptoms appear, disease progression is irreversible, and affected palms typically die within one to two years if young, or within three to five years in mature stands (Kok et al. 2013).

A range of environmental and anthropogenic factors influence both the timing of symptom onset and the rate of disease progression. BSR development is accelerated under poorly drained or waterlogged soils, where elevated moisture and oxygen stress promote fungal activity and root decay (Jazuli et al. 2022). The disease is also more prevalent in acidic soils (pH < 5.5), while near-neutral pH conditions tend to suppress pathogen growth (Rahman and Othman 2020; Goh et al. 2020). The zero-burn replanting system, which retains infected woody residues from previous crops, significantly increases inoculum carry-over and infection risk in new plantings (Siddiqui et al. 2021; Flood et al. 2022). In addition, mechanical root injury from field operations and continuous monocropping enhance pathogen spread via root-to-root contact and shorten the latent infection phase (Paterson 2022; Zakaria 2023). Remote sensing and UAV-based hyperspectral imaging have recently been utilized to detect early physiological changes prior to visible symptom emergence, offering potential for large-scale disease surveillance and risk prediction (Kurihara et al. 2022; Kent et al. 2023).

Collectively, current evidence indicates that *G. boninense*, infection can begin during the seedling or early juvenile phase, but visible symptoms generally manifest between the 4th and 8th year after field establishment, contingent upon soil conditions, inoculum load, and plantation

management. The increasing frequency of early infections observed in replanting cycles underscores the urgent need for improved site sanitation, early detection systems, and integrated disease management strategies to mitigate the long-term impact of BSR on oil palm productivity.

The relationship between soil properties and BSR is crucial for understanding disease dynamics and improving management strategies. Several factors related to soil properties, including nutrient status, pH, and soil type, influence the incidence of BSR. Adequate and balanced soil fertility enhances palm vigor and defence mechanisms, whereas nutrient imbalances and acidity increase vulnerability to pathogen invasion (Goh et al. 2020). Recent studies have shown that phosphorus (P), potassium (K), and magnesium (Mg) deficiencies are frequently associated with higher disease incidence, while optimal nutrition improves root architecture and limits fungal colonization (Yunus et al. 2024; Aziz et al. 2021). Micronutrients such as zinc (Zn) and copper (Cu), when excessive, have been correlated with elevated BSR infection due to oxidative stress and altered enzymatic balance in palm tissues (Ramdan et al. 2023).

Soil pH is particularly significant, as acidic soils (pH 3.4 to 3.9) are linked to higher BSR incidences, especially in coastal and acid sulphate soils where high water retention and clay content stress the palm trees, facilitating pathogen invasion (Parthiban et al. 2016; Goh et al. 2017). Additionally, disease incidence tends to decline in near neutral soils (pH 6.0), where beneficial microbial communities suppress pathogen activity (Goh et al. 2020). Soil organic carbon (SOC) and moisture content also play pivotal roles: high SOC in poorly drained soils maintains inoculum viability, while fluctuating moisture regimes facilitate mycelial spread through root-to-root contact (Aziz et al. 2021; Fitriana et al. 2024). Moreover, studies indicate that micronutrients like zinc, copper, and calcium are associated with greater disease infection, with more than 50% of necrotic bole tissues showing a direct correlation to these elements (Goh et al. 2017).

Recent controlled experiments and field studies have provided quantitative evidence of these relationships. In a controlled environment, *G. boninense* infection in seedlings was significantly affected by soil electrical conductivity (EC) and temperature dynamics, confirming that environmental stress within the rhizosphere modulates pathogen colonization (Aziz et al. 2021). Field surveys further revealed that Spodosols and Histosols, characterized by high organic matter and water-holding capacity, exhibited greater BSR prevalence compared to well-drained sandy soils (Ramdan et al. 2023; Zakaria 2023). Moreover, soil amendment with silicon-enriched fertilizers significantly reduced disease progression, likely due to improved mechanical strength of root tissues and induced systemic resistance (Mayzaitul-Azwa et al. 2025; Goh et al. 2020). These findings underscore that the interplay of soil pH, nutrient balance, and hydrological conditions governs the spatial distribution and temporal development of BSR.

Understanding the influence of soil factors such as nutrient availability, pH, and physical characteristics on the progression of BSR is crucial for developing effective management strategies in oil palm plantations. This study aims to investigate the role of diverse soil properties in influencing BSR development. Specifically, the objective is to assess the relationship between BSR incidence and the variability in soil physical and chemical attributes.

Materials and method

Site description

The study was conducted in two distinct locations in Peninsular Malaysia, namely Seberang Perak, Perak and Kluang, Johor which differ in soil types and environmental conditions relevant to agricultural research, where the area is homogeneity in terms of the practices. Seberang Perak (4° 10′N, 100° 53′E) is characterized by the Jawa Series soils, predominantly found in coastal plains transitioning into peat swamp areas. These soils, classified as part of the Sulfik Tempajelah family (Paramananthan 1998), are poorly drained with a sulfuric horizon occurring at depths of 50–100 cm. Previously mapped as the Selangor Series (shallow phase), they exhibit fine, mixed, isohyperthermic properties. The Seberang Perak study area, illustrated in Fig. 1(a), consists of 64 census points and represents conditions typical of coastal oil palm plantations. In contrast, Kluang (1° 56′N, 103° 22′E) is dominated by the Melaka Series, a highly weathered and leached lateritic soil occurring on hilltops. These soils are well-drained, fine-textured clays with low fertility due to extensive leaching and the presence of ironstone nodules within the subsoil profile (Abdalrahem et al. 2024; Malaysian Soil Taxonomy Update 2018). Formed from iron-rich schist, shale, and phyllite, the Melaka Series is characterized by a low cation exchange capacity. The Kluang study area, shown in Fig. 1(b), includes 42 census points and reflects the agricultural context of the region. In 2007, the site contained 133 oil palm stands, but by 2014, 40% had been felled due to basal stem rot (BSR) infection. Kluang continues to serve as an important site for ongoing oil palm research. Together, these contrasting sites provide valuable insights into soil characteristics and their implications for oil palm cultivation and disease management in Malaysia.



Fig. 1 (**a**) Image of Seberang Perak study area with 64 sampling points (Source: Google Earth, 2015) and (**b**) image of Kluang study area with 42 sampling points (Source: Google Earth, 2014)

Data collections

Assessment of BSR infection was conducted through a systematic census of oil palm trees, with disease symptoms carefully documented. The census assessment was conducted by trained experts from the Malaysian Palm Oil Board (MPOB). During the field survey, any palm exhibiting visible symptoms associated with basal stem rot (BSR) such as yellowing, wilting, unopened spears, or canopy deformation was classified as an unhealthy or infected palm, while asymptomatic palms were recorded as healthy. According to Flood et al. (2022), symptoms typically include multiple unopened spear leaves, crown flattening, and one-sided canopy thinning, all reflecting compromised water and nutrient supply due to basal decay, fractured old fronds, and the presence of fungal fruiting bodies on the trunk. Confirmation of *G. boninense* detection was achieved using the *Ganoderma* Selective Medium (GSM) test, a reliable diagnostic tool for isolating the causal pathogen (Marasas and van der Westhuizen 1996). The integration of visual assessments with GSM confirmation ensured accurate determination of BSR infection (Bakar and Nordin 2011; Dale and Ghazali 2004). Soils were sampled at the end of the fertiliser cycle, two weeks before the next scheduled application (pre-round), with sampling coordinates recorded for georeferencing. This timing avoids short-term spikes from recent applications and yields a representative 'residual' nutrient status under operational conditions. Samples were collected using a soil auger at the same locations where Penetrologger readings were taken, determined via Differential Global Positioning System (DGPS). The penetrologger, equipped with a 1 cm^2 base area and a 60° top angle, measured soil penetration resistance, generating cone index (CI) values in MPa. This parameter reflects the average force exerted by the soil on the conical probe, serving as an indicator of load-bearing capacity and root penetration potential, which are influenced by soil texture, moisture, density, and particle bonding strength.

A semi-grid sampling design was employed, with samples collected at each censused palm to capture spatial variability in BSR occurrence. Samples were stored in sealed containers, transported to the laboratory, oven-dried, and sieved prior to analysis. Physical properties analyzed included cone index (CI), moisture content (MC), and elevation, while chemical analyses were limited to cation exchange capacity (CEC), pH, exchangeable magnesium (Mg), calcium (Ca), potassium (K), available phosphorus (P), sulfur (S), and total carbon (C). Total nitrogen (N) analysis was not discussed in this project. The soil samples were collected before the next fertilization cycle to minimize the influence of recently applied fertilizers (Nelson et al. 2015). This study was limited to the specified soil properties and did not consider other influential factors, including topography, drainage, elevation, and additional environmental variables that may affect overall crop infection.

Data analysis

The data obtained from soil sampling and BSR censusing were analyzed through a combination of statistical analysis and spatial mapping, allowing both numerical and visual interpretation of the relationships between soil attributes and disease infection. Statistical analyses were performed using the Statistical Product and Service Solutions (SPSS) software package. Descriptive statistics, including the minimum, maximum, mean, standard deviation, and coefficient of variation (CV), were first calculated to provide a general overview of the variability and distribution patterns of the

soil parameters. These descriptive measures helped to identify attributes with high variability, which may contribute to uneven soil conditions influencing palm susceptibility to BSR.

To further examine the potential influence of soil nutrients on BSR infection, independent sample t-test was conducted. This analysis assessed whether mean differences in key soil chemical properties, such as exchangeable cations, phosphorus, and organic matter, were statistically significant across different categories of BSR infection. The comparison of nutrient concentrations between healthy and infected palms, particularly macro- and micronutrients like N, K, Ca, Cu, Mn, and B, aimed to identify specific soil nutrient profiles associated with either disease suppression or susceptibility to BSR (Idris et al. 2016). By comparing nutrient concentrations between healthy and infected palms, the t-test provided insights into whether specific soil nutrients could be associated with either disease suppression or disease susceptibility. This t-test approach enabled the identification of only those soil variables that contributed meaningfully to observed differences, thereby improving the reliability of the interpretation.

In parallel with the statistical analysis, visual mapping of soil attributes and BSR infection was conducted using ArcGIS 10.1. Soil variability maps were developed using kriging and interpolation techniques, which are widely recognized for their accuracy in representing continuous spatial data. This geostatistical method, particularly ordinary kriging, allows for the prediction of attribute values at unsampled locations based on surrounding measured values, thereby creating continuous surfaces that depict the spatial distribution of each element (Rebi et al. 2023). These maps were then overlaid with BSR distribution maps, where palm health status was categorized into two main groups: healthy and infected. This classification was necessary due to the relatively small sample size of confirmed BSR-affected palms, but still allowed for meaningful spatial interpretation of disease incidence. The infection of BSR was visualized on a gradient scale, ranging from healthy palms with no visible symptoms to severely infected palms at risk of death. To facilitate interpretation, soil variability maps were divided into five distinct zones using the quantile classification method in ArcGIS, ensuring an even distribution of values within each class interval. This zoning highlighted localized "hotspots" of soil nutrient imbalances and allowed visual comparison with disease distribution patterns.

By integrating statistical testing with spatial mapping, the study combined quantitative rigor with spatial visualization. This dual approach strengthened the robustness of the findings by enabling both numerical evaluation and pattern recognition. The statistical analyses established whether observed differences in soil nutrients were significant, while the spatial maps provided a practical representation of how soil variability coincided with BSR occurrence in the field. Together, these methods facilitated a more comprehensive understanding of the interactions between soil characteristics and BSR incidence, offering valuable insights for targeted soil and disease management in oil palm plantations.

Results and discussion

Descriptive statistic

The descriptive statistics of soil physicochemical properties for both Seberang Perak ($n=64$) and Kluang ($n=42$) are presented in Tables 1 and 2, respectively. Substantial spatial and chemical variability was observed between the two sites, reflecting differences in soil genesis, texture, and landform position. In Seberang Perak, which represents the coastal alluvial plain, soils were characterized by moderate moisture content (mean = 36.77%), slightly acidic pH (mean = 4.68), and medium cation-exchange capacity (CEC) averaging 14.44 cmol/kg. Macronutrient concentrations

Table 1 Descriptive statistics of various soil properties in Seberang Perak

Parameters	Range	Min	Max	Mean	Std. Dev.	Variance	CV
MC (%)	37.10	20.40	57.50	36.77	7.23	52.29	19.67
Elev. (m)	10.05	9.10	19.15	13.04	2.12	4.49	16.25
C (%)	0.39	1.11	1.50	1.28	0.10	0.01	7.77
CEC (cmol/kg)	2.70	13.29	15.99	14.44	0.81	0.66	5.61
Cu (cmol/kg)	6.04	0.54	6.58	1.75	2.13	4.52	121.80
K (cmol/kg)	0.60	1.18	1.78	1.38	0.13	0.02	9.09
Mg (cmol/kg)	1.20	1.46	2.66	2.01	0.40	0.16	19.69
Zn (cmol/kg)	1.94	1.19	3.13	2.06	0.53	0.28	25.48
S (%)	0.03	0.02	0.05	0.03	0.01	0.00	16.65
pH	0.53	4.47	5.00	4.68	0.15	0.02	3.23
CI (MPa)	61.62	123.72	185.34	159.79	16.22	263.12	10.15
P (ppm)	23.02	12.00	35.02	19.55	6.80	46.24	34.79

Note: Number of samples (n) = 64

Table 2 Descriptive statistics of various soil properties in Kluang

Parameters	Range	Min	Max	Mean	Std. Dev	Variance	CV
Elev. (m)	12.65	62.5	75.14	70.1	3.41	11.6	4.86
pH	1.47	3.67	5.14	4.19	0.38	0.14	9.08
CEC (cmol/kg)	24.4	2.6	27	10.96	5.04	25.37	45.97
Ca (cmol/kg)	1.84	0.1	1.94	0.54	0.32	0.1	59.76
Mg (cmol/kg)	0.95	0.04	0.99	0.25	0.2	0.04	78.29
K (cmol/kg)	0.69	0.1	0.79	0.38	0.18	0.03	47.94
P (ppm)	315.35	4.66	320	54.08	68.77	4729.57	127.17
C (%)	3.53	0.56	4.09	1.71	0.76	0.57	44.07

Note: Number of samples (n) = 42

were generally moderate, with mean K and Mg values of 1.38 cmol/kg and 2.01 cmol/kg, respectively, while available P averaged 19.55 ppm but exhibited the highest spatial variation (CV = 34.79%). Micronutrients such as Cu and Zn were more heterogeneous where CV = 121.8% and 25.5%, respectively. Overall, the relatively uniform pH and CEC indicate stable soil chemistry, whereas high variability in P and Cu suggests inconsistent nutrient cycling and possible influences of waterlogging and organic residue decomposition typical of coastal acid sulphate and alluvial soils (Shamshuddin et al. 2014). In contrast, the Kluang site situated on inland lateritic uplands dominated by the Melaka soil series showed stronger acidity (mean pH = 4.19) and lower nutrient retention capacity (mean CEC = 10.96 cmol/kg) compared with Seberang Perak. Macronutrient levels were markedly lower, with mean Ca, Mg, and K concentrations of 0.54, 0.25, and 0.38 cmol/kg, respectively, while available P was highly variable (range = 4.66–320 ppm; CV = 127.17%), indicating strong spatial heterogeneity. Mean organic C (1.71%) was relatively low. While, the high coefficients of variation for Ca, Mg, K, and P (ranging from 47.9% to 127.2%) indicate substantial nutrient heterogeneity, which may influence localized plant nutrient uptake. Collectively, the comparison between the two sites demonstrates that Seberang Perak soils are relatively more fertile, well-buffered, and homogeneous, while Kluang soils are more acidic, nutrient-poor, and spatially variable.

Normality test

Assessment of data normality was conducted to ensure compliance with the assumptions of parametric testing. The Shapiro–Wilk test was selected because it is widely regarded as one of the most powerful and reliable normality tests, especially for small and unequal sample sizes in detecting non-normal distributions (Razali and Wah 2011).

Shapiro–Wilk tests indicated that the assumption of normality was partially met across the soil properties analyzed, with clearer deviations observed in the infected zone compared to the healthy zone (Table 3). In the healthy zone (Class 1, $n = 12$), most soil properties were approximately normally distributed ($p > 0.05$), including moisture content (MC), elevation, carbon (C), cation exchange capacity (CEC), potassium (K), zinc (Zn), soil pH, cone index (CI), and available phosphorus (P). These results suggest relatively homogeneous conditions within healthy soils. However, copper (Cu), magnesium (Mg), and sulphur (S) showed significant departures from normality ($p < 0.05$), indicating skewed distributions or the presence of outliers for these micronutrients.

In contrast, the infected zone (Class 2, $n = 52$) exhibited more widespread deviations from normality. Shapiro–Wilk results showed significant non-normal distributions ($p < 0.05$) for MC, elevation, C, CEC, Cu, K, Mg, Zn, S, pH, and P, reflecting greater heterogeneity in soil properties under diseased conditions. Only cone index (CI) did not deviate significantly from normality ($p = 0.055$), suggesting a relatively symmetric distribution for soil compaction in infected areas.

For Kluang area, in the healthy zone, several soil properties were approximately normally distributed ($p > 0.05$), including carbon (C), potassium (K), elevation, and, marginally, soil pH. In contrast, available phosphorus (P), calcium (Ca), magnesium (Mg), cation exchange capacity (CEC), and soil pH showed significant deviations from normality ($p < 0.05$), indicating skewed distributions or potential outliers in these parameters (Table 4). For the infected zone, fewer variables satisfied the normality assumption. Carbon (C), potassium (K), calcium (Ca), and soil pH did not show significant deviations from normality ($p > 0.05$), suggesting approximately normal distributions for these properties. Conversely, available phosphorus (P), magnesium (Mg), cation exchange capacity (CEC), and elevation exhibited significant non-normality ($p < 0.05$), reflecting increased variability under infected conditions.

Overall, the Shapiro–Wilk results indicate that normality assumptions were only partially satisfied for soil properties in Kluang, with non-normal distributions observed in both healthy and infected zones. Compared with Seberang Perak, Kluang soils showed less extreme but still notable departures from normality, particularly for nutrient-related parameters such as P, Mg, and CEC.

Table 3 Test of normality for various soil properties in Seberang Perak

Parameters	Class	Kolmogorov-Smirnov[a]			Shapiro-Wilk		
		Statistic	df	Sig.	Statistic	df	Sig.
MC (%)	1.00	0.161	12	0.200*	0.945	12	0.563
	2.00	0.15	52	0.005	0.94	52	0.011
Elev. (m)	1.00	0.199	12	0.200*	0.906	12	0.191
	2.00	0.135	52	0.019	0.953	52	0.04
C (%)	1.00	0.16	12	0.200*	0.951	12	0.647
	2.00	0.173	52	0	0.929	52	0.004
CEC (cmol/kg)	1.00	0.192	12	0.200*	0.888	12	0.11
	2.00	0.15	52	0.005	0.906	52	0.001
Cu (cmol/kg)	1.00	0.428	12	0	0.602	12	0
	2.00	0.436	52	0	0.505	52	0
K (cmol/kg)	1.00	0.159	12	0.200*	0.943	12	0.541
	2.00	0.123	52	0.046	0.919	52	0.002
Mg (cmol/kg)	1.00	0.309	12	0.002	0.774	12	0.005
	2.00	0.236	52	0	0.861	52	0
Zn (cmol/kg)	1.00	0.133	12	0.200*	0.96	12	0.781
	2.00	0.113	52	0.093	0.937	52	0.008
S (%)	1.00	0.417	12	0	0.608	12	0
	2.00	0.459	52	0	0.581	52	0
pH	1.00	0.128	12	0.200*	0.954	12	0.696
	2.00	0.154	52	0.003	0.899	52	0
CI (MPa)	1.00	0.116	12	0.200*	0.951	12	0.658
	2.00	0.086	52	0.200*	0.956	52	0.055
P (ppm)	1.00	0.184	12	0.200*	0.869	12	0.063
	2.00	0.197	52	0	0.879	52	0

*This is a lower bound of the true significance

[a]Lilliefors Significance Correction

Table 4 Test of normality for various soil properties in Kluang

Parameters	Reclass	Kolmogorov-Smirnov[a]			Shapiro-Wilk		
		Statistic	df	Sig.	Statistic	df	Sig.
C (%)	1.00	0.125	20	0.200*	0.920	20	0.098
	2.00	0.172	22	0.089	0.894	22	0.023
P (ppm)	1.00	0.297	20	0.000	0.743	20	0.000
	2.00	0.304	22	0.000	0.705	22	0.000
K (cmol/kg)	1.00	0.156	20	0.200*	0.930	20	0.157
	2.00	0.211	22	0.012	0.918	22	0.071
Ca (cmol/kg)	1.00	0.132	20	0.200*	0.836	20	0.003
	2.00	0.152	22	0.200*	0.953	22	0.358
Mg (cmol/kg)	1.00	0.159	20	0.198	0.872	20	0.013
	2.00	0.230	22	0.004	0.746	22	0.000
CEC (cmol/kg)	1.00	0.195	20	0.044	0.893	20	0.030
	2.00	0.199	22	0.023	0.906	22	0.040
pH	1.00	0.189	20	0.059	0.875	20	0.015
	2.00	0.177	22	0.071	0.918	22	0.068
Elev. (m)	1.00	0.143	20	0.200*	0.945	20	0.299
	2.00	0.237	22	0.002	0.852	22	0.004

*This is a lower bound of the true significance

[a]Lilliefors Significance Correction

Table 5 Test of homogeneity of variances for various soil properties in Seberang Perak

Parameters	Levene's Test for Homogeneity of Variances	F	df1	df2	Sig.
MC (%)	Based on Mean	0.055	1	62	0.816
Elev. (m)	Based on Mean	0.901	1	62	0.346
C (%)	Based on Mean	6.142	1	62	0.016
CEC (cmol/kg)	Based on Mean	0.767	1	62	0.385
Cu (cmol/kg)	Based on Mean	1.768	1	62	0.188
K (cmol/kg)	Based on Mean	0.012	1	62	0.912
Mg (cmol/kg)	Based on Mean	0.764	1	62	0.385
Zn (cmol/kg)	Based on Mean	11.947	1	62	0.001
S (%)	Based on Mean	0.759	1	62	0.387
pH	Based on Mean	2.122	1	62	0.150
CI (MPa)	Based on Mean	0.098	1	62	0.755
P (ppm)	Based on Mean	26.521	1	62	0.000

Note: Number of samples (n) = 64

These deviations are typical of field-based soil datasets and likely reflect spatial heterogeneity and localized management or disease effects. Given the moderate and relatively balanced sample sizes in Kluang (n = 20–22), parametric analyses were retained, supported by the robustness of the t-test to moderate violations of normality. Effect size estimation using Hedges' g was therefore used to complement hypothesis testing and to provide a meaningful assessment of the magnitude of differences between healthy and infected zones.

Homogeneity of variances

Levene's test for homogeneity of variances was conducted to evaluate the equality of variance among soil physicochemical parameters between healthy and infected palm in Seberang Perak (Table 5). The test results revealed that most soil parameters exhibited non-significant variance differences ($p > 0.05$), indicating that the assumption of homogeneity was met. Specifically, soil moisture content (MC) ($p = 0.816$), elevation ($p = 0.346$), cation exchange capacity (CEC) ($p = 0.385$), copper (Cu) ($p = 0.188$), potassium (K) ($p = 0.912$), magnesium (Mg) ($p = 0.385$), sulfur (S) ($p = 0.387$), pH ($p = 0.150$), and cone index (CI) ($p = 0.755$) all demonstrated homogeneity of variances between the two classes. This indicates relatively consistent spatial distribution and management across healthy and infected zones for these properties. In contrast, total carbon (C) ($F = 6.142$, $p = 0.016$), zinc (Zn) ($F = 11.947$, $p = 0.001$), and phosphorus (P) ($F = 26.521$, $p < 0.001$), exhibited significant variance heterogeneity ($p < 0.05$). The unequal variances in these parameters suggest strong spatial variability, likely influenced by site-specific fertilizer practices, differential organic matter decomposition, and micro-topographic effects in the coastal alluvial landscape. The large heterogeneity observed in P may also reflect non-uniform fertilizer distribution and varying nutrient leaching intensity across micro zones, as previously reported in Malaysian oil palm plantations on marine clay soils (Anuar et al. 2008; Tan et al. 2016).

Table 6 Test of homogeneity of variances for various soil properties in Kluang

Parameters	Levene's Test for Homogeneity of Variances	F	df1	df2	Sig.
C (%)	Based on Mean	4.833	1	40	0.034
P (ppm)	Based on Mean	11.225	1	40	0.002
K (cmol/kg)	Based on Mean	1.665	1	40	0.204
Ca (cmol/kg)	Based on Mean	2.97	1	40	0.093
Mg (cmol/kg)	Based on Mean	2.333	1	40	0.135
CEC (cmol/kg)	Based on Mean	2.957	1	40	0.093
pH	Based on Mean	0.29	1	40	0.593
Elev. (m)	Based on Mean	0.662	1	40	0.421

Note: Number of samples (n) = 42

In Kluang, among the soil chemical properties tested, the assumption of homogeneity of variances was violated for total carbon (C) ($F = 4.833$, $p = 0.034$) and available phosphorus (P) ($F = 11.225$, $p = 0.002$), where $p < 0.05$ indicates significant differences in group variances as shown in Table 6. This suggests unequal variability in these parameters between healthy and infected palms. For all other soil variables potassium (K), calcium (Ca), magnesium (Mg), cation exchange capacity (CEC), pH, and elevation, it was shown that the Levene's test returned $p > 0.05$, indicating that the assumption of homogeneity was met. These findings indicate that, except for C and P, the variance in soil nutrient concentrations between healthy and infected palms was relatively consistent across the sampling sites in Kluang. The heterogeneity observed in C and P may reflect greater spatial or biological variability of these elements within the soil matrix influenced by disease status and root activity. Previous work documents significant spatial heterogeneity for soil organic C and available P in plantation systems, attributable to operational zones, root-zone processes and management legacy (Behera et al. 2016; Wong et al. 2020).

Statistical analysis (t-test)

The oil palm trees were classified into two categories: healthy (Class 1) and BSR-infected (Class 2). In Seberang Perak, statistical comparisons of soil nutrient contents revealed significant differences in cation exchange capacity (CEC), magnesium (Mg), cone index (Cl), and phosphorus (P) between the two groups, as summarized in Table 7. In Kluang, however, only Mg exhibited a significant difference between healthy and infected stands, as shown in Table 8. Results from Levene's test for homogeneity of variance and the independent t-test for mean comparison are presented

Table 7 Comparison of soil properties in infected zone in Seberang Perak between healthy and infected points

Element	Levene's Test for Equality of Variances		t-test for Equality of Means						
	F	Sig.	t	df	Sig. (2-tailed)	Mean Diff.	Std. Error Diff.	95% Confidence Interval of the Diff.	
								Lower	Upper
MC (%)	0.055	0.816	−0.349	62	0.728	−0.815	2.332	−5.477	3.847
Elev. (m)	0.901	0.346	−0.970	62	0.336	−0.659	0.679	−2.016	0.699
C (%)	6.142	0.016	0.687	62	0.494	0.022	0.032	−0.042	0.086
CEC (cmol/kg)	0.767	0.385	2.789	62	0.007	0.687	0.246	0.195	1.179
Cu (cmol/kg)	1.768	0.188	0.868	62	0.389	0.592	0.682	−0.772	1.956
K (cmol/kg)	0.012	0.912	1.203	62	0.234	0.048	0.040	−0.032	0.128
Mg (cmol/kg)	0.764	0.385	2.005	62	0.049	0.248	0.124	0.001	0.496
Zn (cmol/kg)	11.947	0.001	−1.410	62	0.163	−0.235	0.167	−0.569	0.098
S (%)	0.759	0.387	1.057	62	0.295	0.002	0.002	−0.002	0.005
pH	2.122	0.150	0.739	62	0.463	0.036	0.049	−0.061	0.133
CI (MPa)	0.098	0.755	−2.627	62	0.011	−13.049	4.968	−22.979	−3.119
P (ppm)	26.521	0.000	−2.835	62	0.006	−5.856	2.066	−9.985	−1.727

Note: Number of samples (n) = 64

Table 8 Comparison of soil properties in infected zone in Kluang between healthy and infected points

Element	Levene's Test for Equality of Variances		t-test for Equality of Means						
	F	Sig.	t	df	Sig. (2-tailed)	Mean Diff.	Std. Error Diff.	95% Confidence Interval of the Diff.	
								Lower	Upper
C (%)	4.833	0.034	1.391	40	0.172	0.321	0.231	−0.146	0.788
P (ppm)	11.225	0.002	1.715	40	0.094	35.609	20.762	−6.352	77.570
K (cmol/kg)	1.666	0.204	1.706	40	0.096	0.095	0.056	−0.018	0.207
Ca (cmol/kg)	2.97	0.093	1.802	40	0.079	0.174	0.096	−0.021	0.368
Mg (cmol/kg)	2.331	0.135	2.183	40	0.035	0.128	0.058	0.009	0.246
CEC (cmol/kg)	2.957	0.093	1.776	40	0.083	2.694	1.517	−0.372	5.760
pH	0.29	0.593	−0.063	40	0.95	−0.007	0.119	−0.248	0.233
Elev. (m)	0.661	0.421	−0.913	40	0.367	−0.963	1.054	−3.094	1.168

Note: Number of samples (n) = 42

in Tables 5 and 6, respectively. Despite differences in soil types between Seberang Perak and Kluang, Mg consistently emerged as a distinguishing nutrient between healthy and infected palms. Magnesium is physiologically essential, serving as the central atom in chlorophyll molecules and contributing to cation–anion balance, which regulates cellular pH. Deficiency in Mg is known to increase starch and dry matter accumulation in older leaves, fruits, grains, and roots, potentially explaining the observed variations between healthy and infected palms (Sugianto et al. 2023). These findings highlight magnesium as a critical soil parameter for assessing oil palm health and suggest its potential as an indicator for early detection of BSR infection.

Effect size analysis

In addition to hypothesis testing, effect size analysis was conducted using Hedges' g to quantify the magnitude of differences in soil properties between healthy and infected zones. While p-values indicate whether a statistically significant difference exists, they do not convey the practical or biological importance of that difference. Effect size measures provide a standardized estimate of the magnitude of group differences that is independent of the units of measurement and facilitates meaningful interpretation of soil–plant interactions. Hedges' g was selected in preference to Cohen's d because it incorporates a correction factor that reduces small-sample bias and provides a more accurate estimate of the standardized mean difference when sample sizes are unequal or relatively small, as in the present study (Lakens 2013). For independent samples comparisons, Hedges' g was calculated by dividing the mean difference between groups by the pooled standard deviation and applying a bias-correction factor.

Effect size analysis using Hedges' g revealed large differences between healthy and infected zones for cation exchange capacity (g = 0.88), cone index (g = −0.83), and available phosphorus (g = −0.90) in Seberang Perak as

Table 9 Comparison of size differences between healthy and infected zones in Seberang Perak

Parameter	SD pooled	Cohen's d	J factor	Hedges' g	Magnitude
MC (%)	7.282	−0.112	0.988	−0.111	Small
Elev. (m)	2.12	−0.311	0.988	−0.307	Small–Medium
C (%)	0.1	0.22	0.988	0.218	Small
CEC (cmol/kg)	0.768	0.894	0.988	0.884	Large
Cu (cmol/kg)	2.13	0.278	0.988	0.275	Small
K (cmol/kg)	0.125	0.384	0.988	0.38	Small–Medium
Mg (cmol/kg)	0.387	0.641	0.988	0.633	Medium
Zn (cmol/kg)	0.521	−0.451	0.988	−0.445	Small-Medium
S (%)	0.006	0.32	0.988	0.316	Small–Medium
pH	0.153	0.235	0.988	0.232	Small
CI (MPa)	15.513	−0.841	0.988	−0.831	Large
P (ppm)	6.451	−0.908	0.988	−0.897	Large

Note: Number of healthy samples (n1) = 52, Number of infected samples (n2) = 12

Table 10 Comparison of size differences between healthy and infected zones in Kluang

Parameter	SD pooled	Cohen's d	J factor	Hedges' g	Magnitude
C (%)	0.748	0.429	0.981	0.421	Small-Medium
P (ppm)	67.2	0.53	0.981	0.52	Medium
K (cmol/kg)	0.181	0.524	0.981	0.514	Medium
Ca (cmol/kg)	0.311	0.56	0.981	0.549	Medium
Mg (cmol/kg)	0.188	0.682	0.981	0.669	Medium
CEC (cmol/kg)	4.91	0.549	0.981	0.538	Medium
pH	0.385	−0.018	0.981	−0.018	Negligible
Elev. (m)	3.411	−0.282	0.981	−0.277	Small

Note: Number of healthy samples (n1) = 20, Number of infected samples (n2) = 22

shown in Table 9. In addition, magnesium (Mg) exhibited a medium effect size (g = 0.63), indicating a meaningful difference between groups. Collectively, these results suggest that infection is associated with substantial alterations in soil nutrient availability and physical properties, underscoring their practical and biological significance despite variability in statistical significance across parameters.

Effect size analysis showed small to medium differences in soil properties between healthy and infected zones in Kluang (Table 10). Among the nutrients analyzed, magnesium (Mg) exhibited the largest effect size (g = 0.669), indicating a comparatively stronger and biologically meaningful response to infection status. Given its critical role in plant nutrition and cation balance, Mg was therefore highlighted as a key parameter in assessing soil health differences.

Semivariogram analysis

The semivariogram results (Table 11) show that most soil properties at Seberang Perak exhibit strong spatial dependence, as indicated by low nugget-to-sill ratios (< 0.25) and high determination coefficients ($R^2 > 0.90$). Macronutrients such as P, K, Mg, and CEC showed moderate to large spatial ranges (71–223 m) and high predictive accuracy ($R^2 = 0.95–0.98$), indicating that their variability is well-structured and suitable for kriging interpolation. Zn also displayed a large spatial range (349 m) with excellent model performance, suggesting strong continuity across the field. In contrast, variables such as Cu and soil pH demonstrated shorter spatial ranges (33–44.5 m) but still produced acceptable cross-validation results, reflecting localized but predictable variation. Soil moisture content (MC) and sulphur (S) exhibited very short ranges (11 m and 1.11 m), indicating weak spatial structure and high micro-scale variability; thus, kriging predictions for these variables should be interpreted with caution. The compaction index (CI) showed moderate spatial dependence (111 m) with good model performance ($R^2 = 0.88$). Overall, the fitted exponential, spherical, and Gaussian models accurately represent the spatial behaviour of each nutrient, confirming the suitability of geostatistical interpolation (e.g., kriging) for generating reliable soil properties map for precision management in the study area (Li & Heap, 2014).

Table 11 Semivariogram model based on the geo-statistical analysis for the soil properties in Seberang Perak

Element	Model	Nugget (Co)	Co+C (Sill)	Co/(Co+C)	Range (Ao)	R^2	RSS
C (%)	Exponential	0.0001	0.0143	0.00698	41.2	0.907	2.63×10^{-5}
P (ppm)	Exponential	0.1000	70.2000	0.00142	89.1	0.954	4.6×10^{-2}
K (cmol/kg)	Spherical	1.00	2862	0.00035	124.7	0.964	3.8×10^{-5}
Mg (cmol/kg)	Gaussian	10.00	3966	0.00252	71.2	0.976	6.3×10^{-5}
CEC (cmol/kg)	Gaussian	0.45	1.6980	0.265	222.6	0.955	0.0369
pH	Gaussian	0.00	0.0293	0.00034	44.5	0.982	3.29×10^{-5}
MC (%)	Exponential	9.50	51.1	0.18591	11.1	0.898	10278
Cu (cmol/kg)	Exponential	0.0100	6.6420	0.00151	33.4	0.844	11.2
Zn (cmol/kg)	Exponential	1.0000	1.3090	0.76394	349.2	0.966	8.15×10^{-3}
S (%)	Exponential	0.0000	0.0000	0.00000	1.11	0.289	2.77×10^{-10}
CI (MPa)	Gaussian	20.6	412.900	0.05	111.3	0.884	30771

Note: Number of samples (n) = 64

Table 12 Semivariogram model based on the geo-statistical analysis for the soil properties in Kluang

Element	Model	Nugget (Co)	Co+C (Sill)	Co/(Co+C)	Range (Ao)	R^2	RSS
C (%)	Gaussian	0.001	0.545	0.00183	19.3	0.623	0.157
P (ppm)	Linear	6987.67	6987.67	1.00000	99.27	0.181	1.5×10^{9}
K (cmol/kg)	Linear	0.03586	0.03586	1.00000	99.27	0.168	1.469×10^{-4}
Ca (cmol/kg)	Gaussian	0.0001	0.1162	0.00086	16.7	0.743	5.113×10^{-3}
Mg (cmol/kg)	Gaussian	0.0029	0.04	0.928	19.3	0.622	2.797×10^{-4}
CEC (cmol/kg)	Exponential	0.09	23.56	0.996	12.8	0.021	298
pH	Exponential	0.0388	0.1746	0.222	8.5	0.339	8.13×10^{-3}
Elev. (m)	Gaussian	0.35	16.42	0.0213	173.6	0.95	6.71

Note: Number of samples (n) = 42

Table 13 Cross-validation results based on the geo-statistical analysis for the soil properties in Seberang Perak

Variable	ME	RMSE	R^2	RMSSE	Mean Kriging SD
Mg (cmol/kg)	−0.0027	0.072	0.966	0.015	5.51
P (ppm)	−0.0937	2.81	0.827	0.774	3.41
CEC (cmol/kg)	−0.0062	0.365	0.849	0.515	0.7
CI (MPa)	−0.0024	9.04	0.689	1.72	5.22

Note: Number of samples (n) = 64

Table 14 Cross-validation results based on the geo-statistical analysis for the soil properties in Kluang

Variable	ME	RMSE	R^2	RMSSE	Mean Kriging SD
Mg (cmol/kg)	−0.0006	0.205	0.0085	1.16	0.17

Note: Number of samples (n) = 42

The semivariogram parameters in Table 12 indicate varying spatial structures among the measured soil properties in Kluang. Most variables fitted Gaussian and Exponential models, showing moderate to strong spatial dependence, while P and K followed a Linear model with nugget-to-sill ratios of 1.0, implying a lack of spatial continuity and purely random variation across the study area (Khan et al. 2021). The semivariogram of CEC show high proportion suggests very weak spatial dependence and implies that CEC values are dominated by micro-scale variation or measurement noise rather than structured spatial continuity. In addition, the low model performance ($R^2 = 0.021$) and high residual error (RSS = 298) indicate poor variogram fit and weak predictive reliability. In contrast, C, Ca and Mg exhibited very low nugget-to-sill ratios (<0.01), suggesting strong spatial dependence and that their variability is mainly governed by intrinsic soil factors. The range values (8.5–19.3 m) for these elements indicate that their spatial correlation extends only over moderate distances, reflecting localized variability typical of heterogeneous agricultural soils. pH showed moderate model performance ($R^2 = 0.339$), suggesting non-spatial or random variability, while elevation demonstrated strong spatial continuity ($R^2 = 0.95$) with a large range (173.6 m), confirming its gradual topographic variation across the field. Overall, the results highlight that key soil nutrients (Ca, Mg, and C) possess structured spatial patterns suitable for geostatistical interpolation, whereas CEC, P and K exhibit irregular distribution likely influenced by management or sampling factors.

Cross-validation analysis

Cross-validation analyses were conducted for both the Seberang Perak and Kluang areas (Table 13). However, only Mg, P, CEC, and CI from the Seberang Perak area and Mg from the Kluang area were selected as priority parameters that showed significant differences between infected and healthy palms. The results for Seberang Perak (Table 10) indicate that the ordinary interpolation models performed well, with low mean error (−0.0027 to −0.0937) and RMSE values, confirming minimal bias and high prediction accuracy. Mg showed the strongest performance ($R^2 = 0.966$; RMSE = 0.072 cmol/kg), demonstrating excellent spatial predictability (Tajudin et al. 2016). P and CEC also performed well ($R^2 = 0.827$ and 0.849, respectively), reflecting consistent short-range spatial dependence typical of tropical soils with variable nutrient fixation. Cone index (CI) showed lower accuracy ($R^2 = 0.689$) but still captured meaningful spatial trends linked to soil compaction and drainage variation. Overall, high R^2 values (0.689–0.966) and near-zero bias confirm that the variogram models effectively describe the spatial structure of key soil properties. These outcomes validate the reliability of interpolation-based maps for BSR risk zoning in oil palm plantations.

For the Kluang site, the ordinary kriging cross-validation for Mg produced a mean error (ME) of −0.00066 cmol/kg, indicating that the model was essentially unbiased (Table 14). Although the root mean square error (RMSE) was 0.205 cmol/kg, this value appears relatively large when compared with the narrow distribution of Mg values in the dataset. Consequently, the coefficient of determination from cross-validation ($R^2 = 0.0085$) appeared low, not because the model lacked spatial structure, but because the natural

variability of Mg was small. This behavior is common in soil nutrient datasets where limited variation causes classical R^2 values to underestimate predictive accuracy (Bhunia et al. 2018; Shahidin et al. 2022). Consistent with this, the semivariogram analysis showed a clear spatial structure for Mg, with a good model fit ($R^2 = 0.622$) and a moderate range of 19.3 m, indicating localized spatial dependence. However, when the prediction error (RMSE) is of similar magnitude to the mean and standard deviation, the cross-validation R^2 naturally becomes small even when the geostatistical model is valid. Therefore, the Mg kriging maps should be interpreted qualitatively, useful for identifying relative spatial patterns but not intended for precise pointwise quantitative prediction.

Distribution map analysis

Figure 2(a) presents the interpolation map distinguishing healthy and BSR infected oil palms, with healthy areas (green) concentrated from the northern to central region, and infected areas (pink) extending from the centre towards the south. The spatial patterns of Mg (Fig. 2b) and CEC (Fig. 2c) show that low concentrations (1.48–1.96 cmol/kg for Mg and 13.29–14.23 cmol/kg for CEC) are mainly distributed in the western to southern zones, whereas higher concentrations (2.25–2.70 cmol/kg for Mg and 14.84–15.99 cmol/kg for CEC) occur in the northern to eastern zones. These low Mg and CEC concentrations largely coincide with the infected regions identified in Fig. 2(a). In contrast, the distribution of P (Fig. 2d) reveals lower levels in the northern to southeastern zones and higher levels in the east to south. Furthermore, Fig. 2(e) demonstrates that approximately 80% of high CI values (1.59–1.93 MPa) are concentrated within the infected area. Similarly, the spatial distribution in Kluang (Fig. 3a) shows that nearly half of the study area is affected by BSR. Low Mg concentrations (0.05–0.28 cmol/kg) dominate about 80% of the region (Fig. 3b), with higher Mg levels (0.37–0.96 cmol/kg) confined to localized patches. Comparison with the healthy-infected map (Fig. 3a) indicates a strong association between low Mg zones and infected stands. Consistent with the t-test results (Tables 7 and 8), Mg emerges as the only soil nutrient capable of reliably differentiating between healthy and infected oil palms in Kluang.

Conclusion

This study demonstrated the strong relationship between soil nutrient status and the incidence of BSR in oil palm plantations, with Seberang Perak and Kluang selected as representative sites due to their documented BSR outbreaks. Independent t-test analyses revealed that Mg, P, CEC, and CI significantly differentiated between healthy and infected areas in Seberang Perak, while Mg alone showed significant differences in Kluang. Notably, spatial variability maps of Mg closely reflected the distribution of infected crop in both study areas, underscoring the role of Mg as a consistent indicator of infection. This trend was evident across different soil series (Jawa and Melaka), suggesting that Mg deficiency may be intrinsically linked to BSR susceptibility. In Seberang Perak, located on acid sulfate Jawa Series soils, significant differences in CEC, Mg, CI, and available P between healthy and infected palms reflect poor nutrient-retention capacity and Fe/Al-oxide dominance typical of acid-sulfate environments (Karananidi et al. 2022; Abdalrahem et al. 2024). The acid sulfate nature of Jawa Series soils further constrains root respiration, and in combination with shallow water tables and periodic flooding, provides a favourable micro-environment for *G. boninense* development (Khoo and Chong 2023). The lower CI indicates softer, less-stable topsoil consistent with root decay and prolonged saturation, both conducive to *G. boninense* colonisation (Khoo and Chong 2023). In contrast, the Kluang site, under well-drained lateritic Melaka Series soils, exhibited only Mg as significantly different, while Ca, K, and P were marginally lower in infected plots. Such patterns typify highly weathered kaolinitic soils with low base saturation and strong Fe/Al-oxide fixation (Abdalrahem et al. 2024). The cross-validation analysis for the Kluang area indicated a weakness in the kriging method for generating the spatial variability map. This limitation was mainly due to the low variability of the Mg data and the very short spatial range observed in the semivariogram, which prevented kriging from capturing any meaningful spatial structure. Under such conditions, the Inverse Distance Weighting (IDW) method provides a more reliable interpolation approach because it does not depend on variogram modelling and performs better when spatial autocorrelation is weak or absent (Ouabo et al. 2020). These findings demonstrate the potential of soil nutrient assessment, especially magnesium (Mg) concentration, as an effective diagnostic indicator for the early detection of basal stem rot (BSR), consistent with observations reported in previous studies (Mahmud and Chong 2022; Yunus et al. 2024; Zakaria 2023). Such an approach can provide valuable guidance for pre-replanting evaluations and support more targeted disease management strategies. Furthermore, integrating soil nutrient mapping with digital technologies, such as Internet of Things (IoT) based monitoring, could enhance the precision and scalability of BSR detection. Future research should expand the investigation to include a wider range of soil types and varying levels of BSR incidence, thereby refining the robustness and applicability of nutrient-based diagnostic methods. Ultimately,

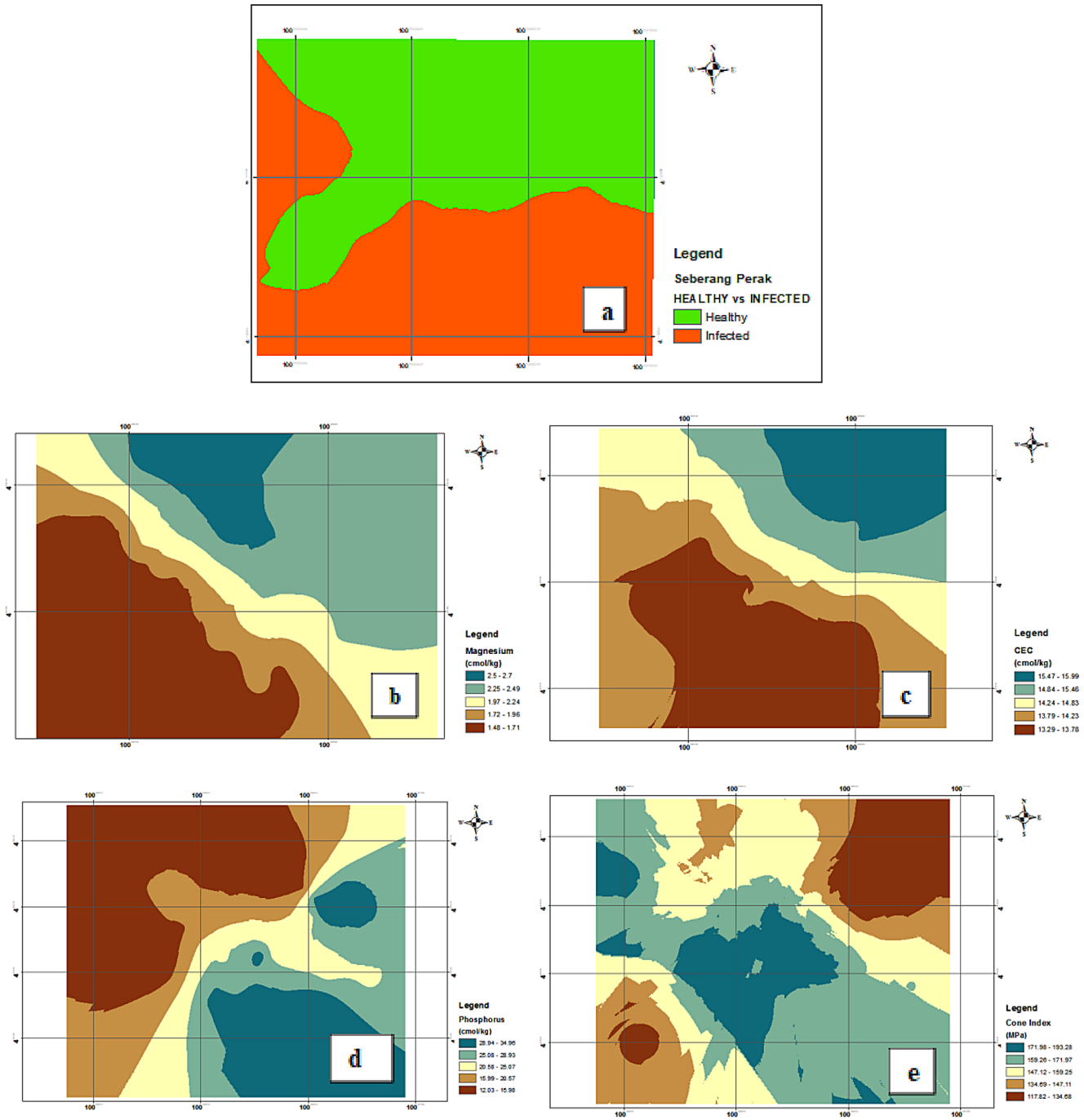


Fig. 2 Variability maps for (**a**) healthy and infected crop distribution, (**b**) Mg, (**c**) CEC, (**d**) P and (**e**) CI in Seberang Perak

these insights contribute to more sustainable and informed management of oil palm plantations under the persistent challenge of BSR.

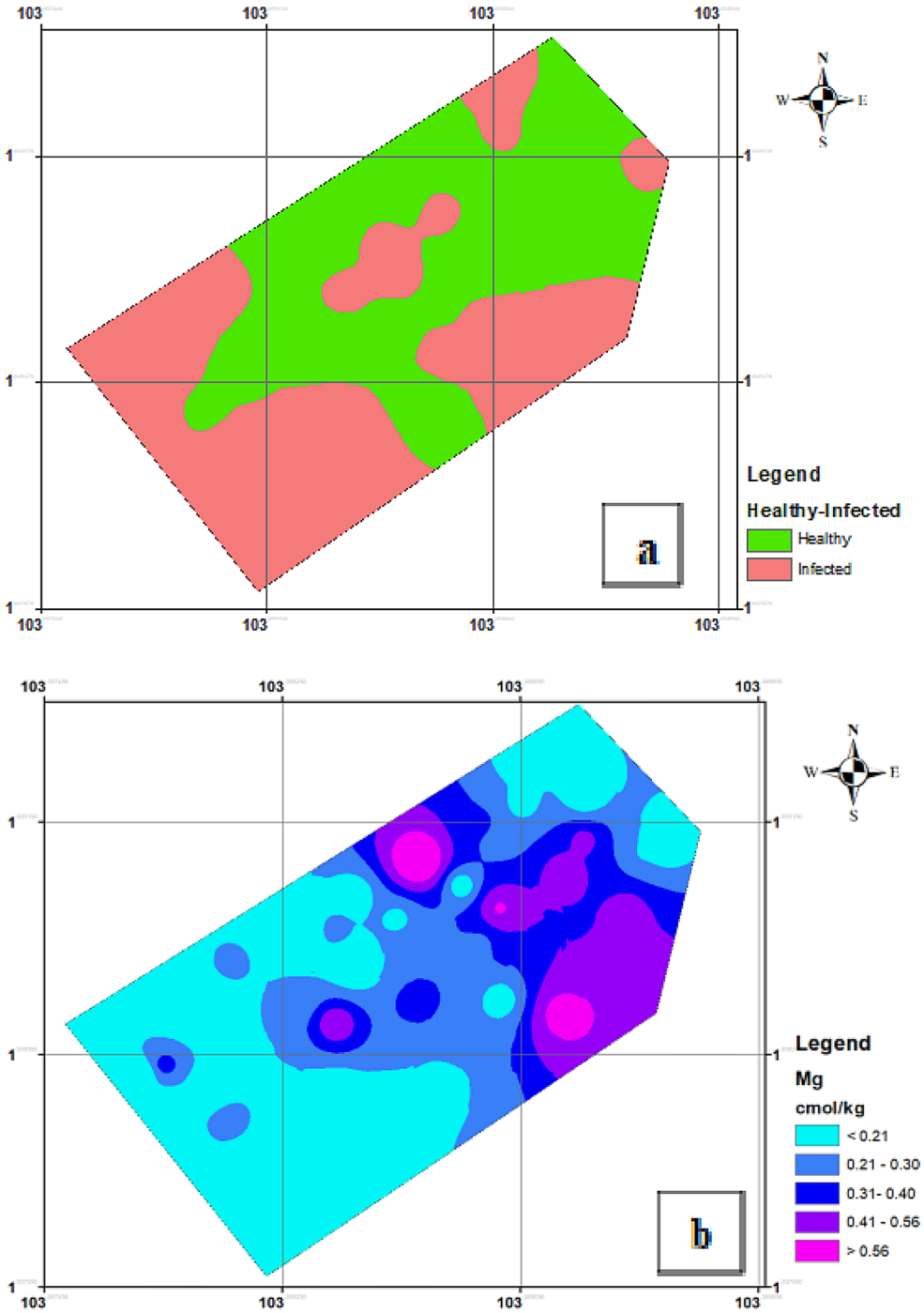


Fig. 3 Variability maps for (**a**) healthy and infected crop distribution and (**b**) Mg in Kluang

Acknowledgements This work was supported by the Universiti Putra Malaysia [UPM/PSP/GPPP/2024/9110016]. Thank you to all staffs who have contributed to the research.

Funding Open access funding provided by The Ministry of Higher Education Malaysia and Universiti Putra Malaysia. This work was supported by the Universiti Putra Malaysia (Grant number UPM/PSP/GPPP/2024/9110016).

Data availability The datasets generated during and/or analysed during the current study are available from the corresponding author on reasonable request.

Declarations

Ethical approval This study does not need any ethical approval.

Conflicts of interest The authors have no financial or proprietary interests in any material discussed in this article. The remaining authors declare that the research was conducted in the absence of any commercial or financial relationships that could be construed as a potential conflict of interest.

Open Access This article is licensed under a Creative Commons Attribution 4.0 International License, which permits use, sharing,

adaptation, distribution and reproduction in any medium or format, as long as you give appropriate credit to the original author(s) and the source, provide a link to the Creative Commons licence, and indicate if changes were made. The images or other third party material in this article are included in the article's Creative Commons licence, unless indicated otherwise in a credit line to the material. If material is not included in the article's Creative Commons licence and your intended use is not permitted by statutory regulation or exceeds the permitted use, you will need to obtain permission directly from the copyright holder. To view a copy of this licence, visit http://creativecommons.org/licenses/by/4.0/.

References

Journal articles

Abdalrahem OM, Khairunniza-Bejo S, Wayayok A, Hashim F (2024) Effect of slope, aspect and position on soil properties at different soil depths under oil palm plantations. MSc Thesis, Universiti Putra Malaysia

Anuar AR, Goh KJ, Heoh TB, Ahmed OH (2008) Spatial variability of soil inorganic N in a mature oil palm plantation in Sabah, Malaysia. Am J Appl Sci 5(9):1239–1246

Aziz MHA, Khairunniza-Bejo S, Wayayok A, Hashim F, Kondo N (2021) Temporal changes analysis of soil properties associated with *G. boninse* infection in oil palm seedlings. Agronomy 11(11):2279

Bakar SK, Nordin MS (2011) Characterization of basal stem rot disease in oil palm: symptoms and management strategies. J Plant Pathol 93:523–530

Behera SK, Rao BN, Suresh K, Manoja K (2016) Soil nutrient status and leaf nutrient norms in oil palm (Elaeis guineensis Jacq.) plantations grown on the Southern Plateau of India. Proc Natl Acad Sci India Sect B Biol Sci 86(3):691–697

Bhunia GS, Shit PK, Chattopadhyay R (2018) Assessment of spatial variability of soil properties using geostatistical approaches in a lateritic soil region of West Bengal, India. Ann Agrarian Sci 16(4):436–443

Dale MA, Ghazali R (2004) Symptoms and causes of basal stem rot in oil palm plantations in Southeast Asia. Oil Palm Res 9:4558

Fitriana CDA, Wirianata H, Astuti YMT, Wilisiani F, Sukarman S, Primananda S, Utami WP (2024) Macronutrient interactions and microbial population in Ultisols and Spodosols affecting the incidence of *Ganoderma* disease. Pertanika J Sci Technol 32(S4):23–38

Flood J, Bridge PD, Pilotti CA (2022) Basal stem rot of oil palm revisited. Ann Appl Biol 181(2):160–181

Goh YK, Lim CK, Cheng CR, Tan SY, Cheah LW, Ah Tung PG, Goh YK, Goh KJ (2017) Effects of chemical properties of different soils on *Ganoderma* disease in oil palm (Elaeis guineensis). Oil Palm Bull 75:17–26

Goh YK, Md Zoqratt MZH, Goh YK, Ayub Q, Ting ASY (2020) Determining soil microbial communities and their influence on *Ganoderma* disease incidences in oil palm (Elaeis guineensis) via high-throughput sequencing. Biology 9(12):424

Hardini PA, Prakoso AB, Medina S, Baskara G, Wandri R, Asmono D, Suwandri S, Subandiyah S, Muslim A (2025) Identification and pathogenicity of Ganoderma causing basal stem rot in oil palm in South Sumatra. Int J Agriculture Biol 25:657–665

Hushiarian R, Yusof NA, Dutse SW (2013) Detection and control of *Ganoderma boninense*: strategies and perspectives. SpringerPlus 2(555):1–12

Idris AS, Sijam K, Ahmad K, Ibrahim MS, Hashim Z, Seman IA (2016) Leaf nutrient status in relation to severity of Ganoderma infection in oil palm seedlings artificially infected with Ganoderma boninense using root inoculation technique. Agric Food Sci, Environ Sci

Jazuli NA, Zareen S, Ramle M (2022) A review of factors affecting basal stem rot incidence in oil palm plantations. Plants 11(10):1345

Karananidi P, Valente T, Braga MAS, Reepei M, Pechy MINF, Wang Z, Bachmann RT, Jusop S, Md Som A (2022) Acid sulfate soils decrease surface water quality in coastal area of West Malaysia: Quo Vadis? Geoderma Reg 28:e00467

Kent OW et al (2023) Early symptom detection of basal stem rot disease in oil palm trees using a deep learning approach on UAV images. Comput Electron Agric 211:107979

Khan MZ, Islam MR, Salam ABA, Ray T (2021) Spatial variability and geostatistical analysis of soil properties in the diversified cropping regions of Bangladesh using geographic information system techniques. Appl Environ Soil Sci 2021:6639180

Khoo YW, Chong KP (2023) *Ganoderma boninense*: general characteristics of pathogenicity and methods of control. Front Plant Sci 14:1156869

Kok SM, Goh YK, Tung HJ, Goh KJ, Wong WC, Goh YK (2013) In vitro growth of *Ganoderma boninense* isolates on novel palm extract medium and virulence on oil palm (Elaeis guineensis) seedlings. Malays J Microbiol 9(1):33–42

Kurihara J, Koo V-C, Guey CW, Lee YP, Abidin H (2022) Early detection of basal stem rot disease in oil palm tree using unmanned aerial vehicle-based hyperspectral imaging. Remote Sens 14(3):799

Li,J., & Heap, A.D. (2014). Spatial interpolation methods applied in the environmental sciences: A review. Environmental Modelling & Software, 53, 173-189.

Mahmud MS, Chong KP (2022) Effects of liming on soil properties and its roles in increasing the productivity and profitability of the oil palm industry in Malaysia. Agriculture 12(3):322

Malaysian Soil Taxonomy Update (2018) Classification and morphological characteristics of major soil series in Peninsular Malaysia. Department of Agriculture Malaysia, Putrajaya

Marasas WFO, van der Westhuizen GC (1996) The *Ganoderma* selective medium (GSM) test for diagnosing basal stem rot in oil palm. Plant Dis 80:1033–1036

Mayzaitul-Azwa NJ, Shuhada NMT, Hanafi MM, Huda N (2025) Impact of silicon-enriched fertilizer on basal stem rot disease in palm species caused by *Ganoderma boninense*. Pertanika J Trop Agric Sci 48(3):973–990

Nelson PN, Banabas M, Goodrick I, Webb MJ, Huth NI, O'Grady D (2015) Soil sampling in oil palm plantations: a practical design that accounts for lateral variability at the tree scale. Plant Soil 394(1–2):421–429

Nusaibah SA, Siti nor Akmar A, Idris AS, Sariah M, Mohamad Pauzi Z (2016) Involvement of metabolites in early defense mechanism of oil palm (Elaeis guineensis Jacq.) against *Ganoderma* disease. Plant Physiol Biochem 109:156–165

Ouabo RE, Sangodoyin AY, Ogundiran MB (2020) Assessment of ordinary kriging and inverse distance weighting methods for modeling chromium and cadmium soil pollution in e-waste sites in Douala, Cameroon. J Health Pollut 10(26):200605

Parthiban K, Vanitah R, Jusoff K, Nordiana AA, Anuar AR, Wahid O, Hamidah AB (2016) GIS mapping of basal stem rot disease in relation to soil series among oil palm smallholders. Am J Agric Biol Sci 11:2.12

Paterson RRM (2022) Longitudinal trends of future suitable climate for conserving oil palm indicate refuges in tropical south-east Asia with comparisons to Africa and south America. Pac Conserv Biol 28(1):57–67

Rahman KA, Othman R (2020) Influence of pH levels on disease development in oil palm seedling roots infected with *Ganoderma boninensis*. Rhizosphere 13:1–4

Ramdan EP, Hartono A, Giyanto, Hidayat S, Widodo (2023) The relationship between soil fertility and basal stem rot disease in oil palm plantations. Agrosainstek 7(1):32–39

Razali NM, Wah YB (2011) Power comparisons of shapiro-wilk, Kolmogorov-Smirnov, lilliefors and anderson-darling tests. J Stat Model Anal 2(1):21–33

Rozieta R, Sahibin AR, Wan Mohd Razi I (2015) Physico-chemical properties of soil at oil palm plantation area, Labu, Negeri Sembilan. AIP Conf Proc 1678:020031

Shahidin NM, Roslan I, Zaharah SS, Kang SH, Elisa AA, Malisa MN, Kamarudin KN, Murano H, Abe SS (2022) Soil spatial variation in a sloping mango orchard of Northern Peninsular Malaysia. Malays J Soil Sci 26:104–119

Shamshuddin J, Azura AE, Shazana MARS, Fauziah CI, Panhwar QA, Naher UA (2014) Chapter three - properties and management of acid sulfate soils in Southeast Asia for sustainable cultivation of rice, oil palm, and cocoa. In: Advances in agronomy, vol 124. Elsevier, pp 91–142

Siddiqui Y, Meon S, Ahmad R (2021) Advances in early detection and management of *Ganoderma* basal stem rot in oil palm plantations. Saudi J Biol Sci 28(12):7011–7024

Sugianto H, Monzon JP, Pradiko I, Tenorio FA, Lim YL, Donough CR, Sunawan S, Rahutomo S, Agus F, Cock J, Amsar J, Farrasati R, Iskandar R, Edreira JIR, Saleh S, Santoso H, Tito AP, Ulfaria N, Slingerland MA, Grassini P (2023) First things first: widespread nutrient deficiencies limit yields in smallholder oil palm fields. Agric Syst 210:103709

Tajudin NSM, Musa MH, Abu Seman I, Halim MS (2016) Determination and mapping of calcium and magnesium contents using geostatistical techniques in oil palm plantation related to basal stem rot disease. Songklanakarin J Sci Technol 38(1):23–30

Tan NP, Wong MK, Yusuyin Y, Abdu AB, Iwasaki K, Zaharah AR, Tanaka S (2016) Distribution of soil P fractions in oil palm plantation of different planting ages in Pahang, Malaysia [Poster presentation]. In Soil Science Society Conference (SPS 2016). Universiti Putra Malaysia

Wong MK, Selliah P, Ng TF, Hassan MHA, Van Ranst E, Inubushi K (2020) Impact of agricultural land use on physicochemical properties of soils derived from sedimentary rocks in Malaysia. Soil Sci Plant Nutr 66(1):214–224

Yunus NSM, Muhamad Tajudin NS, Johari SN, Rosham Kadiman NM (2024) Evaluation of oil palm leaf nutrients affected by *Ganoderma* disease. Revelation Sci 1(2):92–103

Zakaria L (2023) Basal stem rot of oil palm: the pathogen, disease incidence and control methods. Plant Dis 107(3):603–615

Articles by DOI

Karunaratna SC, Patabendige NM, Lu W, Asad S, Hapuarachchi KK (2024) An in-depth study of phytopathogenic ganoderma: pathogenicity, advanced detection techniques, control strategies, and sustainable management. J Fungi 10(6):414. https://doi.org/10.3390/jof10060414

Lakens D (2013) Calculating and reporting effect sizes to facilitate cumulative science: a practical primer for t-tests and ANOVAs. Front Phychol 4:863. https://doi.org/10.3389/fpsyg.2013.00863

Leng STK, Cheah WY, Pahri S-DR, Lin NS, Choy EA (2024) A systematic literature review on environmental issues and challenges towards the palm oil industry. J Sustainability Sci Manag 19(1):154–170. https://doi.org/10.46754/jssm.2024.01.013

MPOB (Malaysian Palm Oil Board) (2024) Malaysian oil palm statistics 2024. MPOB, Kuala Lumpur. Retrieved from https://bepi.mpob.gov.my/images/overview/Overview2024.pdf

Murphy DJ, Goggin K, Paterson RRM (2021) Oil palm in the, 2020s, and beyond: challenges and solutions. CABI Agric Biosci 2:39. https://doi.org/10.1186/s43170-021-00058-3

Paterson RRM (2019) *Ganoderma boninense* disease deduced from simulation modelling with large data sets of future Malaysian oil palm climate. Phytoparasitica. https://doi.org/10.1007/s12600-019-00723-4

Rebi A, Wang G, Hussain A, Flynn T, Ullah H, Chenghao Z, Jamil M, Afzal A, Khan MUH, Ahmed MI, Zhou J (2023) Spatial distribution and quantification of plant-available nutrients and soil properties in Punjab, Pakistan. Research Square (Preprint). https://doi.org/10.21203/rs.3.rs-3622450/v1

Santoso H, Yusuf MA, Rahutomo S, Madiyanto, Winarna (2024) A cutting-edge precision agriculture technology to support the sustainable oil palm industry. IOP Conf Ser Earth Environ Sci 1308(1):012053. https://doi.org/10.1088/1755-1315/1308/1/012053

Books

Fageria NK (2016b) The use of nutrients in crop plants. CRC Press, Boca Raton

Book chapter

Soepena H, Purba RY, Pawirosukarto (2000) A control strategy for basal stem rot (ganoderma) on oil palm. In: Ganoderma diseases of perennial crops, vol 2000. CAB International, pp 83–88

Bulletin/report

Paramananthan S (1998) Malaysian soil taxonomy (second approximation): a proposal for the classification of Malaysian soils. In: Malaysian Soc Soil Sci, Param Agricultural and Soil Surveys (M) Sdn. Bhd., Kuala Lumpur, Malaysia

Publisher's Note Springer Nature remains neutral with regard to jurisdictional claims in published maps and institutional affiliations.